

Photovoltaic Performance of BHJ Organic Solar Cells Based on Incorporation of Ru Dye into P3HT:PCBM Matrix

Fatih ONGÜL*¹

¹Yıldız Technical University, Faculty of Arts and Sciences, Department of Physics, 34210, Istanbul/Turkey

(Alınış / Received: 20.02.2017, Kabul / Accepted: 07.07.2017, Online Yayınlanma / Published Online: 01.08.2017)

Keywords

Ru-N719,
P3HT,
PCBM,
BHJ,
Organic solar cells

Abstract: In this study, spin coating method was used for fabricating the P3HT:PCBM bulk heterojunction organic photovoltaic (OPV) devices comprising of Ru dye at different concentrations. The effects of Ru dye incorporated into P3HT:PCBM matrix on photovoltaic and diode parameters of the devices were investigated. It was observed that incorporating Ru dye with the lowest concentration into ternary system, improved the device performance, whereas device performance decreased with the increasing concentration of Ru dye in the blend of ternary system. The power conversion efficiency of OPV device was enhanced about 10% with incorporating Ru dye.

Ru Boyanın P3HT:PCBM Matrisine Dahil Edilmesine Dayanan BHJ Organik Güneş Pillerinin Fotovoltaik Performansı

Anahtar Kelimeler

Ru-N719,
P3HT,
PCBM,
BHJ,
Organik güneş pilleri

Özet: Bu çalışmada, farklı konsantrasyonlarda Ru boya içeren P3HT:PCBM hacim heteroeklem organik güneş pilleri dönel kaplama yöntemi ile üretilmiştir. P3HT:PCBM matrisine dahil edilen Ru boyasının aygıtların fotovoltaik ve diyot parametrelerine olan etkileri araştırılmıştır. Cihaz performansının üçlü sistemde en düşük konsantrasyona sahip Ru boyası eklenmesiyle geliştiği, buna karşılık Ru boya konsantrasyonunun üçlü sistem karışımında daha da arttırıldığında, cihazların fotovoltaik performansının azaldığı gözlenmiştir. OPV cihazının güç dönüşüm verimliliği Ru boya dahil edilerek yaklaşık %10 arttırılmıştır.

1. Introduction

The world currently consumes heavily fossil fuels, which are non-renewable for their energy sources. Day by day, the finite resources are gradually decreasing and as a result of decrease they are getting too expensive. In addition to this, they have harmful effects on the environment. In contrast to fossil fuels, the renewable energy resources such as solar energy will never run out and always provide clean power [1].

Solar cells made from inorganic, organic materials or their combinations have attracted enormous attention [2-3]. Organic photovoltaic (OPV) devices have grown in importance due to their tuneable properties and low production costs, and being flexible and easy to be processed. However, organic photovoltaic devices have certain disadvantages such as low efficiency and short lifetime as compared to inorganic photovoltaic devices. Thereof, researchers make a great effort to develop new polymeric

materials, new combinations and structures to enhance the efficiency. The most commonly used concept for organic solar cells is the bulk heterojunction (BHJ) in which an electron donor and an electron acceptor material are blended together. The BHJ concept provides larger interface area between donor and acceptor materials [4-8].

Ru metal complexes as a sensitizer have been widely used in dye-sensitized solar cells (DSSCs) because of their favorable properties such as wide absorption range, suitable energy levels and high stability [9-11]. Besides, Ru dyes have been used in organic solar cells in order to modify the interface between electron transport layer such as TiO₂ and electron-donor polymer [12-15]. Di-tetrabutylammonium cis-bis(isothiocyanato) bis(2,2'-bipyridyl-4,4'-dicarboxylato) ruthenium(II) (N-719) is the most popular Ru dye for DSSCs and OPVs. The energy levels of N719 (LUMO ~3.7 eV and HOMO ~5.5 eV) are suitable for LUMO level (~3.7 eV) of [6,6]-phenyl C61 butyric acid methyl ester (PCBM) and HOMO

level (~5.2 eV) of poly [3-hexylthiophene-2, 5-diyl] (P3HT) (Figure 1). In this study, BHJs based on the ternary system with P3HT, PCBM and Ru N719 with different ratios were prepared for improving the photovoltaic performance of organic solar cells. The effect of concentrations of Ru-N719 on photovoltaic and diode parameters of devices with ITO/PEDOT:PSS/P3HT:PCBM:Ru/Al configuration were investigated (Figure 1).

2. Material and Method

Kintec Company's Indium Tin Oxide (ITO) coated glasses having sheet resistance of 12 Ω/sq and thicknesses of 120 nm were used as substrates. The one-third of ITO with size of 1.5 x 1.5 cm² were patterned by etching with an acid solution (HCl:HNO₃:H₂O) and then cleaned with helmanex solution, deionized water, acetone and isopropyl alcohol in an ultrasonic bath for 20 minutes each step respectively. The solution of poly(3,4-ethylenedioxythiophene) : poly(styrenesulfonate) (PEDOT:PSS, Clevios PH1000) was filtered with 0.45 μm Whatman filter. PEDOT:PSS were coated on ITO substrates by spin coating at 1500 rpm for 60 sec and then samples were dried on a hot plate at 150°C for 4 min in under ambient conditions for removing any residual moisture. The thickness of hole transport layer was ~50 nm.

The solutions of ternary blends were prepared with P3HT from Rieke Metals, PCBM from Solenne and Ru Dye (N719) with various ratios by dissolving in 1 ml chlorobenzene (CB). The ternary blends of P3HT:PCBM:Ru solutions were coated by the spin-casting method onto the PEDOT:PSS layers at 800 rpm for 60 s and the coated samples were annealed at 120°C for 3 min. under atmospheric condition. The thickness of active layer was ~80 nm. Lastly, Aluminium (Al) having thickness of 100 nm was coated with thermal evaporation method under vacuum (1 10⁻⁵ mbar) on top of the active layers.

A computer programmed Keithley 2400 source meter was used for examining current-voltage characteristics of the photovoltaic devices in dark and under the illumination provided by Lutzchem solar simulator set at 100 mW/cm² (AM1.5G) and calibrated by standard crystalline silicon diode. In order to characterize the photovoltaic performance of devices, the illuminated current density-voltage (J-V) curves used for determining open-circuit photovoltage (V_{oc}), short-circuit photocurrent density (J_{sc}), fill-factor FF and parasitic resistances which include the shunt resistance (R_{sh}) and the series resistance (R_s). The ratio of maximum points of V_{max} and J_{max} to the product of V_{oc} and J_{sc} (Equation 1) gives the Fill factor (FF). Besides, the ratio of output power from the solar cell to the input power (P_{in}, 100 mW/cm²) (Equation 2) gives the power conversion efficiency in percent (η_{AM1.5}).

$$FF = \frac{V_{mpp} \times J_{mpp}}{V_{oc} \times J_{sc}} \quad (1)$$

$$\eta_{AM1.5}(\%) = \left(\frac{P_{out}}{P_{in}} \right) \times 100 = \frac{FF \times V_{oc} \times J_{sc}}{P_{in}} \times 100 \quad (2)$$

The general diode equation is expressed as Equation 3 [16].

$$J = J_o \left[\exp \left(\frac{qV}{nk_bT} \right) - 1 \right] \quad (3)$$

Where J_o is the dark saturation current density, q is the elementary charge, V is the voltage, n is the ideality factor, k_b is the Boltzmann's constant and T is the absolute temperature.

The potential barrier height was calculated with the Equation 4.

$$J_o = A^* T^2 \exp \left(-\frac{q\phi_b}{k_bT} \right) \quad (4)$$

Here, A* is the effective Richardson coefficient, T is the absolute temperature, q is the elementary charge, φ_b is the potential barrier height, k_b is the Boltzmann's constant, and J_o is the dark saturation current density which is obtained from the straight line intercept of lnJ at zero potential (V=0) in the dark at room temperature.

The ideality factor was obtained from Equation 5.

$$n = \frac{q}{k_bT} \left(\frac{\partial \ln J}{\partial V} \right)^{-1} \quad (5)$$

New Port Quantum Efficiency System was used for the measurement of incident photon-to-current efficiency (IPCE) of the photovoltaic devices. The theoretical photocurrent density (J_{IPCE}) was determined by integrating the IPCE(λ) spectra over the incident photon flux density using the Equation 6 [17].

$$J_{IPCE} = \int qF(\lambda) IPCE(\lambda) d\lambda \quad (6)$$

Where F(λ) is the photon flux density at AM 1.5 condition, IPCE(λ) is the incident photon-to-current efficiency as a function of wavelength, q is the elementary charge and λ is the wavelength of the incident monochromatic light.

3. Results

The photovoltaic performances of the bulk heterojunction organic solar cells consist of P3HT, PCBM and Ru-N719 with different concentrations were examined. Figure 2 illustrates the current density-voltage curves of these devices with ITO/PEDOT:PSS/P3HT:PCBM:Ru/Al configuration in dark and under illumination.

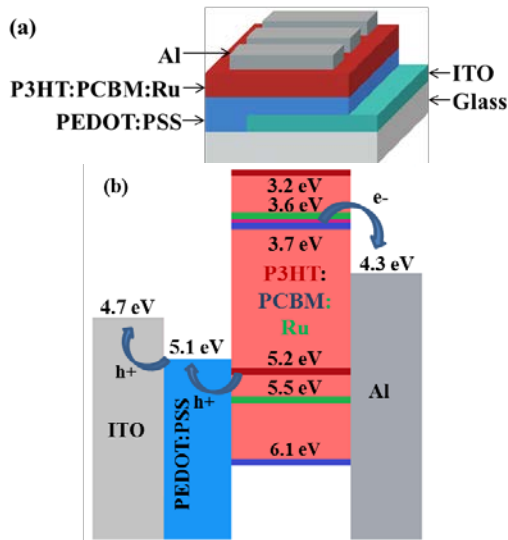


Figure 1. (a) Schematic diagram and (b) energy levels of the components in glass/ITO/PEDOT:PSS/P3HT:PCBM:Ru-N719/Al structure.

Comparison of current density-voltage curves of the devices with different concentrations of Ru dye in ternary system under illumination are shown in Figure 3. The photovoltaic parameters like V_{oc} , J_{sc} , FF, PCE, and also parasitic resistances such as the R_{sh} and R_s determined from the illuminated current density-voltage curves are given in Table 1. The active area of the devices is about 0.1 cm². The control device prepared without Ru-N719 exhibited J_{sc} of 3.0 mA/cm², V_{oc} of 540 mV and FF of 0.4, which led to PCE of 0.63%. The device prepared with incorporating Ru-N719 at 2.5 wt.% concentration into ternary system exhibited J_{sc} of 3.3 mA/cm², V_{oc} of 550 mV and FF of 0.39 leading to PCE of 0.7%. The device performance was improved by incorporating Ru-N719 into ternary system through the increment of J_{sc} in device, which related to the efficiency collection of photogenerated charge carriers at the electrodes. The incorporation of Ru dye with low concentration into P3HT:PCBM matrix could be attributed to better charge extraction between P3HT and PCBM interface. However, as the concentration of Ru-N719 in ternary system was increased from 2.5% to 20%, the efficiencies of the devices decreased up to 0.37% with decrease of J_{sc} from 3.3 to 2.6 mA/cm² and also V_{oc} from 0.55 to 0.50 V. The photovoltaic performances of devices were decreased with the increasing concentration of Ru-N719 in ternary system, which may be caused by recombination of charge carrier at the interface. The shunt resistances of devices were decreased with increasing concentration of Ru, which is related with increasing leakage of current in the active layer. The diode parameters of devices calculated from the dark current density-voltage characteristics indicated a non-ideal diode behavior as shown the ideality factors with 3.88-6.46. The potential barrier height decreased from 0.76 eV to 0.73 eV besides the saturation currents decreased from 1.52×10^{-3} to 5.56×10^{-3} mA/cm² with increasing amount of Ru-N719 when the value of reference device without Ru

were 0.75 eV and 2.76×10^{-3} mA/cm², respectively. The best diode parameters of all devices were obtained by using Ru dye with 2.5% concentration.

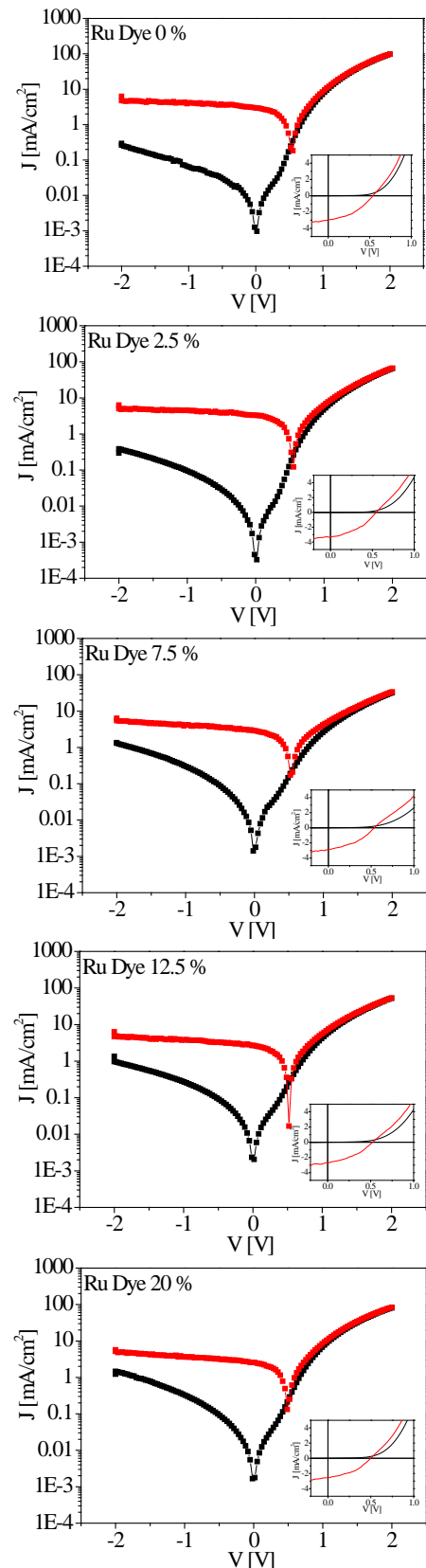
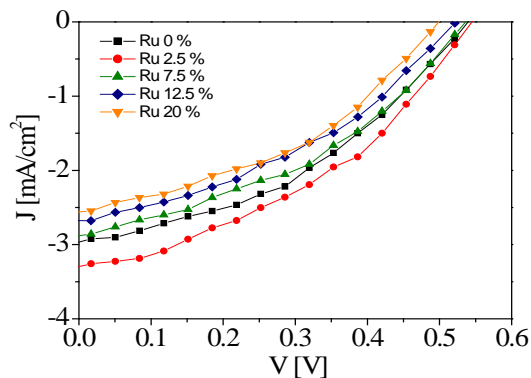
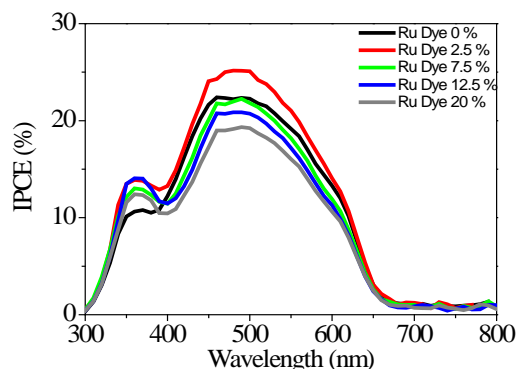


Figure 2. The current density-voltage characteristics of devices based on ternary blends of P3HT:PCBM and Ru Dye with different concentrations (0, 2.5, 7.5, 12.5 and 20 wt.%) in dark and under illumination. The main frames depict the J-V curves in semi-logarithmic scale. The insets show the J-V curves in linear scale.

Table 1. The photovoltaic parameters of devices.

Ru (wt%)	n	ϕ_b (eV)	J_0 dark (mA/cm^2)	V_{oc} (mV)	J_{sc} (mA/cm^2)	J_{IPCE} (mA/cm^2)	FF	PCE (%)	R_s (Ωcm^2)	R_{sh} (Ωcm^2)
0	4.31	0.75	2.8×10^{-3}	540	3.0	2.79	0.40	0.63	92	544
2.5	3.88	0.76	1.5×10^{-3}	550	3.3	3.11	0.39	0.70	83	528
7.5	6.46	0.74	3.4×10^{-3}	530	2.9	2.68	0.40	0.61	95	448
12.5	5.54	0.74	4.1×10^{-3}	520	2.7	2.53	0.38	0.53	101	426
20	4.31	0.74	5.6×10^{-3}	500	2.6	2.36	0.40	0.52	92	467

**Figure 3.** Comparison of current density-voltage curves of the investigated devices in linear scale.**Figure 4.** The IPCE spectra of devices depending on ternary blends of P3HT:PCBM and Ru Dye with different concentrations (0, 2.5, 7.5, 12.5 and 20 wt.%).

The incident photon-to-current conversion efficiency (IPCE) is a measure of the amount of photo-generated carriers collected by the electrodes per incident photon as a function of wavelength. IPCE curve provides detailed information on efficient light harvesting in which portion of solar spectrum for the devices. The IPCE spectra of the devices with different concentrations of Ru dye in ternary system are shown in Figure 4, and also Table 1 illustrates the J_{IPCE} values of these devices calculated using the data of IPCE spectrum. The IPCE curves revealed a broad spectral response that range from 300 to 650 nm. IPCE value of device with incorporating the lowest concentration of Ru dye increased as compared to that of reference device. It can be explained by the improved the total photocurrent which is generated in photoactive layer.

4. Discussion and Conclusion

In summary, the bulk heterojunction organic photovoltaic devices consisting of P3HT, PCBM and Ru-N719 at different concentrations were designed

to improve the photovoltaic parameters of this type OPVs cells. The efficiencies of these BHJ devices ranged from 0.7% to 0.52% based on incorporating the concentration of Ru-N719 into P3HT:PCBM matrix. The device employing the Ru dye with the lowest concentration in ternary system exhibited the best device performance, whereas the photovoltaic performance of devices decreased with increasing concentration of Ru dye in ternary system as compared to control device without Ru dye. The improvement in device performance with increasing J_{sc} may be attributed to improve the exciton harvesting and the photogenerated carrier injection with using the Ru dye in P3HT:PCBM matrix. However, the photovoltaic performances of devices were decreased with the increasing concentration of Ru-N719 in ternary system, which may be caused by charge carrier recombination. In addition, the efficiency of devices affected by high series and low shunt resistances and also saturation currents, barrier heights and ideality factor played a role on the performance were shown in this study.

References

- [1] Panwar N.L., Kaushik S.C., Kothari S. 2011. Role of renewable energy sources in environmental protection: A review, *Renew. Sustain. Energy Rev.* 15, 1513–1524.
- [2] Sangster A.J. 2014. Solar Photovoltaics, *Green Energy Technol.* 194, 145–172.
- [3] Sharma S., Jain K.K., Sharma A. 2015. Solar Cells: In Research and Applications—A Review, *Mater. Sci. Appl.* 06, 1145–1155.
- [4] Gunes S., Neugebauer H., Sariciftci N.S. 2007. Conjugated Polymer-Based Organic Solar Cells, *Chem. Rev.* 107, 1324–1338.
- [5] Scharber M.C., Sariciftci N.S. 2013. Efficiency of bulk-heterojunction organic solar cells, *Prog. Polym. Sci.* 38, 1929–1940.
- [6] Heeger A.J. 2014. 25th anniversary article: Bulk heterojunction solar cells: Understanding the mechanism of operation, *Adv. Mater.* 26, 10–28.
- [7] Lu L., Zheng T., Wu Q., Schneider A.M., Zhao D., Yu L. 2015. Recent Advances in Bulk Heterojunction Polymer Solar Cells, *Chem. Rev.* 115, 12666–12731.
- [8] Dang M.T., Hirsch L., Wantz G. 2011. P3HT:PCBM, Best Seller in Polymer Photovoltaic Research, *Adv. Mater.* 23, 3597–3602.

- [9] Grätzel M. 2005. Solar energy conversion by dye-sensitized photovoltaic cells, *Inorg. Chem.* 44, 6841–6851.
- [10] Hagfeldt A., Boschloo G., Sun L., Kloo L., Pettersson H. 2010. Dye-sensitized solar cells., *Chem. Rev.* 110, 6595–6663.
- [11] Ng T.W., Chan C.Y., Yang Q.D., Wei H.X., Lo M.F., Roy V.A.L. Zhang W.J., Lee C.S. 2013. Charge interaction and interfacial electronic structures in a solid-state dye-sensitized solar cell, *Org. Electron. Physics, Mater. Appl.* 14, 2743–2747.
- [12] Weickert J., Auras F., Bein T., Schmidt-Mende L. 2011. Characterization of interfacial modifiers for hybrid solar cells, *J. Phys. Chem. C.* 115 15081–15088.
- [13] Goh C., Scully S.R., McGehee M.D. 2007. Effects of molecular interface modification in hybrid organic-inorganic photovoltaic cells, *J. Appl. Phys.* 101, 1–12.
- [14] Khatri I., Bao J., Kishi N., Soga T. 2012. Similar Device Architectures for Inverted Organic Solar Cell and Laminated Solid-State Dye-Sensitized Solar Cells, *ISRN Electron.* 180787.
- [15] Chen C.C., Chen L.C. 2012. Study of ruthenium complex sensitizer and gold nanoparticles doped flexible organic solar cells, *Adv. Mater. Sci. Eng.* 206380.
- [16] Sze S. M. 1979. *Physics of Semiconductor Devices*, 3rd ed. John Wiley-Interscience, New York.
- [17] Bisquert J. Garcia-Belmonte G. 2011. On Voltage, Photovoltage, and Photocurrent in Bulk Heterojunction Organic Solar Cells, *J. Phys. Chem. Lett.* 2, 1950–1964.